NAVIER-STOKES PREDICTION OF AERODYNAMIC CHARACTERISTICS OF A 7.62MM SPIN-STABILIZED PROJECTILE AT SUPERSONIC SPEEDS

Bui Xuan Son[1], Do Van Minh[1], Bui Minh Tuan[1], Nguyen Hai Minh[1], Doan Van Dung[1], Nguyen Quang Tuan[1,*]

DOI: http://doi.org/ 10.57001/huih5804.2025.247

ABSTRACT

Accurate prediction of aerodynamic characteristics plays an extremely important role in computing the trajectory of a flying body and analyzing its stability performance. Computational Fluid Dynamics (CFD) has been widely used to predict the aerodynamics of missiles and spinning projectiles. This paper presents the results of numerical determination of aerodynamic characteristics of the 7.62mm M43 projectile at supersonic flight regime with Mach number range from 1.5 to 4.0 at angles of attack varying from 0^0 to 6^0. The aerodynamic characteristics of interest are drag, normal force, overturning moment coefficients and the location of the center of pressure. The Reynolds-averaged Navier-Stokes equations with Shear Stress Transport k-ω turbulence model were employed in this study. The numerical simulations were carried out using Ansys Fluent software. A grid independence study was conducted to ensure that the simulation results do not depend on the grid size. The simulation results were initially validated by comparing with available experimental data to make sure that the applied numerical methodology is accurate and reliable. This research has once more confirmed high effectiveness of CFD method in analyzing the supersonic flow around a spinning projectile. The results obtained in this study can be used in trajectory calculation and stability evaluation of M43 projectile, as well as in the process of modifying or designing new firearms for this kind of projectile. The present paper is a significant contribution to better understanding of aerodynamics of the M43 projectile in particular and spinning projectiles and missiles in general.

Keywords: *CFD, Spin-stabilized projectile, Numerical simulation, Ansys Fluent, Aerodynamic characteristics.*

[1]Faculty of Special Equipment, Le Quy Don Technical University, Vietnam
[*]Email: tuannguyenmta28@gmail.com
Received: 10/5/2025
Revised: 03/7/2025
Accepted: 25/7/2025

1. INTRODUCTION

The 7.62mm M-43 is one of the most widely used projectiles in the world. Currently, the need to design new as well as improve the existing guns to fire M-43 projectiles has gained much attention. However, along with the designing new or improving the existing guns, a crucial problem is to produce new firing tables for them. In order to produce firing tables for a new gun-ammunition system, it is necessary to solve the problem of calculating the trajectory parameters of the projectile. To do this, one must know the aerodynamic characteristics of the projectile at different speeds and angles of attack (AoA) [1]. NATO bloc projectiles have been extensively studied experimentally and numerically. McCoy and Silton have studied the aerodynamic characteristics of the 5.56x45mm projectiles using spark-range firings method [2, 3]. The 7.62x51mm standard and match projectiles have been aerodynamically characterized by McCoy and Maynard [4, 5]. The aerodynamic characterization has been performed for various 12.7mm projectiles by numerous authors [6-9]. DeSpirito and Plostin numerically analysed the damping coefficients of 25mm M910 projectile [10]. The works on aerodynamics of 155mm artillery projectiles have been carried out by a large number of researchers [11-13]. Meanwhile, although the 7.62mm M43 projectile has been designed and used for several decades by multiple armed forces around the world, there has been no published research on its aerodynamics. Therefore, the main objective of this paper is to study the aerodynamic characteristics of M-43 projectile, specifically the drag, normal force and overturning moment coefficients as well as the center of pressure location at supersonic flow conditions. These are

aerodynamic coefficients needed to solve the problems of the external ballistics of a projectile. Currently, to study the aerodynamic characteristics of a flying object, there are some approaches available, namely, experimental methods, semi-empirical methods and CFD methods [14]. The experimental methods include Wind tunnel testing and Free-flight spark range firings. Although these methods provide the most accurate results, they are very time-consuming and resource-expensive. The semi-empirical methods combine experimental data and mathematical tools to represent the aerodynamic characteristics of the object in the form of formulas, graphs, and tables. Even though these methods give quick solutions, they are only applicable to flying objects with simple geometries. Therefore, semi-empirical methods are usually used in the initial design stages. Some popular softwares using semi-empirical methods are PRODAS, AP09, Mc DRAG, Missle Datcom of the US Army [15]. In recent years, with the rapid advancements in computer science and numerical methods, the CFD method has been increasingly employed to study the aerodynamics of flying bodies. In this paper, CFD predictions of aerodynamic characteristics of M-43 projectile in different flow conditions will be undertaken using Ansys Fluent software.

2. COMPUTATIONAL METHODOLOGY

2.1. Model geometry

The geometry model of M-43 projectile used for this research is presented in Fig. 1. The dimensions of the projectile are taken from [16]. The total length of the projectile is 26.62mm. The ogive nose has the length of 15.56mm and radius of 39.50mm. The 9^0-angle boattail has the length of 3.95mm. The diameter of the cylindrical bearing part, or often called the caliber of the projectile, is 7.90mm. The center of gravity of the projectile is located at 15.80mm (2 calibers) from the nose.

The 3D model of the projectile created on CAD Inventor Professional 2021 software is presented in Fig. 2. The 3D model of the projectile was exported into Ansys Fluent software for the subsequent simulation process.

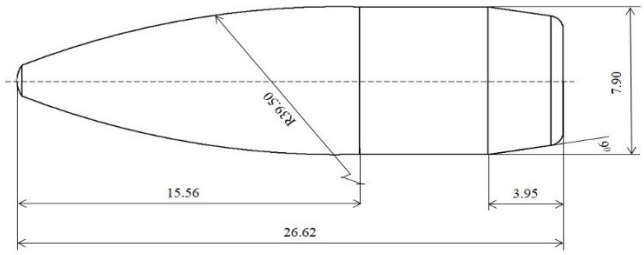

Fig.1. M43 projectile configuration (all dimensions are in mm)

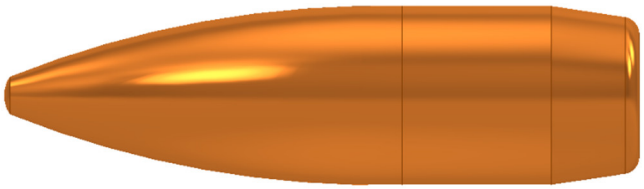

Fig. 2. 3D model of M43 projectile

2.2. Turbulence model

In this study, the Shear Stress Transport (SST) k-ω turbulence model was implemented to simulate the flow around M43 projectile. It was develop by Menter in 1994 [17] and quickly became one of the most widely used turbulence models in scientific researches and industrial applications as well. In essence, the SST k-ω turbulence model is the blending of the standard k-ε and the standard k-ω turbulence models to combine their advantages. The two transport equations are defined as follows:

$$\frac{\partial}{\partial t}(\rho k)+\frac{\partial}{\partial x_i}(\rho k u_i)=\frac{\partial}{\partial x_j}\left(\Gamma_k\frac{\partial k}{\partial x_j}\right)+G_k-Y_k+S_k \quad (1)$$

$$\frac{\partial}{\partial t}(\rho \omega)+\frac{\partial}{\partial x_i}(\rho \omega u_i)=\frac{\partial}{\partial x_j}\left(\Gamma_\omega\frac{\partial \omega}{\partial x_j}\right)+G_\omega-Y_\omega+D_\omega+S_\omega \quad (2)$$

Where G_k is the turbulence kinetic energy due to the mean velocity gradients; G_ω is the generation of ω; Γ_k and Γ_ω are respectively the effective diffusivity of k and ω; Y_k and Y_ω are respectively the dissipations of k and ω due to the turbulence; S_k and S_ω are the user-defined source terms; D_ω is the the cross-diffusion term.

The turbulent viscosity coefficient μ_t is computed as follows:

$$\mu_t=\frac{\rho k \alpha_1}{\max[\alpha_1\omega,\ SF_2]}, \quad (3)$$

where α_1 is a constant of the turbulence model, S is the strain rate magnitude, F_2 is a blending function.

The turbulent Prandtl numbers σ_k and σ_ω in the SST k-ω turbulence model are determined as follows:

$$\sigma_k=\frac{1}{\frac{F_1}{\sigma_{k,1}}+\frac{1-F_1}{\sigma_{k,2}}},\ \sigma_\omega=\frac{1}{\frac{F_1}{\sigma_{\omega,1}}+\frac{1-F_1}{\sigma_{\omega,2}}} \quad (4)$$

where F_1 is a blending function; $\sigma_{k,1}$, $\sigma_{k,2}$, $\sigma_{\omega,1}$, and $\sigma_{\omega,2}$ are constants.

The parameters G_k and G_ω are given as:

$$G_k=\min\left(G_k,10\rho\beta^*k\omega\right),\ G_\omega=\frac{\alpha}{\upsilon_t}G_k \quad (5)$$

where β^* is a constant.

The values of the model constants are: $\sigma_{k,1} = 1.176$, $\sigma_{\omega,1} = 2.0$, $\sigma_{k,2} = 1.0$, $\sigma_{\omega,2} = 1.168$, $\beta_{i,1} = 0.075$, $\beta_{i,2} = 0.0828$, $\beta^* = 0.09$, $k = 0.41$.

2.3. Computational domain

The computational domain was created in a rectangular box shape with length, width and height of 40L, 10L and 10L respectively. Here, L is the total length of the projectile. The computational domain was initialized with a size large enough to fully capture the aerodynamic phenomena occurring near the projectile surface as well as behind the base of the projectile. The projectile model was placed on the symmetrical longitudinal axis of the computational domain and is 15L and 24L away from the Inlet and Outlet boundaries respectively as depicted in Fig. 3.

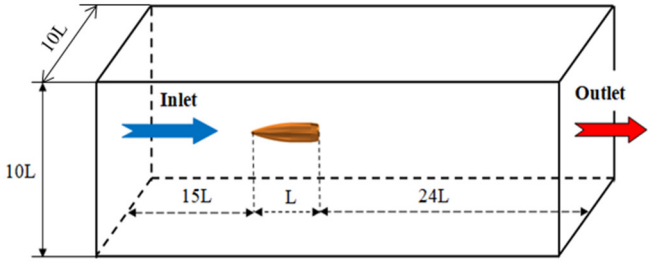

Fig. 3. Computational domain

2.4. Solver setup and boundary conditions

In the present research, the Ansys Fluent software package with SST k-ω turbulence model was employed [18]. The Coupled algorithm was adopted for the study. The air is modelled as ideal gas. The air viscosity model is the three component Sutherland model. The boundary conditions of the computational domain include inlet, outlet, and wall. The Inlet flow was defined as Pressure far field. The Pressure outlet was set for the Outlet boundary condition. The wall was established as non-slip. The atmosphere parameters were set as follows: $p_0 = 101325$Pa and $T_0 = 288.16$K. The simulation result was considered converged once the flow residuals had reduced at least 3 orders of magnitude and the drag varied less than 1% over the last 100 iterations [19].

2.5. Grid independence study

To ensure the simulation results are independent from the grid size, a grid independence study was undertaken. Five grid configurations with different resolutions were created as presented in Table 1 by adjusting the element sizes on the projectile surface and in the remaining simulation domain. Numerical simulations were conducted at the Mach number of 2.0 with the same boundary conditions and solver setup as described above. It can be seen in Table 1 that from the grid size of 6.351 million of cells (Grid 4) the subsequent grid refinement will not affect the simulation result. In addition, the simulated drag coefficient obtained with the Grid 4 is 0.360, meanwhile, the drag value obtained through processing experimental data at the same Mach number is 0.368 [16]. The discrepancy between the simulated and experimental results is only 2.17% indicating the reliability and accuracy of numerical simulation in predicting the aerodynamics of the projectile. Therefore, the Grid 4 was used in this research for predicting aerodynamic characteristics of 7.62mm M43 projectile. The mesh configuration of the computational domain used in this work was presented in Fig. 4.

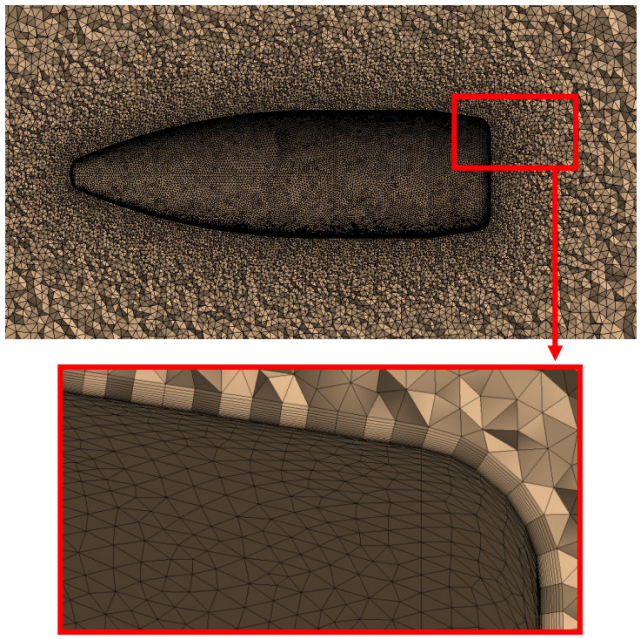

Fig. 4. View of the computational domain mesh (top) and a close-up view of the mesh near the projectile surface with inflation layers (bottom) used in the study

Table 1. Influence of grid size on the simulated drag coefficient at Mach number 2.0

Grid	Number of cells ($x10^6$)	Simulated C_{D0}	Discrepancy with the previous grid (%)
Grid 1	0.438	0.408	-
Grid 2	2.062	0.371	9.07
Grid 3	4.207	0.363	2.16
Grid 4	**6.351**	**0.360**	**0.83**
Grid 5	8.369	0.360	0.00

The grid resolution on the projectile surface was the finest with the maximum element size of 0.15mm and get coarser from the region near the projectile surface to the computation domain boundaries with the maximum element size of 5mm. A 15-layer inflation with the first cell height from the projectile surface of $2.5x10^{-3}$mm and a growth rate of 1.15 was added to ensure that the dimensionless distance y+ is less than 1 to accurately capture the phenomena at the boundary layer.

3. RESULTS AND DISCUSSION

3.1. Aerodynamic characteristics at different Mach numbers and AoA

In this study, in order to access the aerodynamic characteristics of M43 projectile at supersonic flow regime with small yaw, numerical simulations were performed for AoA ranging from 0^0 to 6^0 with an increment of 2^0 at Mach number varying in the interval from 1.5 to 4.0 with an increment of 0.5. The aerodynamic characteristics of interest are zero-yaw and total drag coefficients C_{D0} and C_D, normal force and overturning moment coefficients $C_{N\alpha}$ and $C_{M\alpha}$, as well as center of pressure location X_{cp}. Their variations as functions of Mach number and AoA are shown in Fig. 5 to Fig. 10.

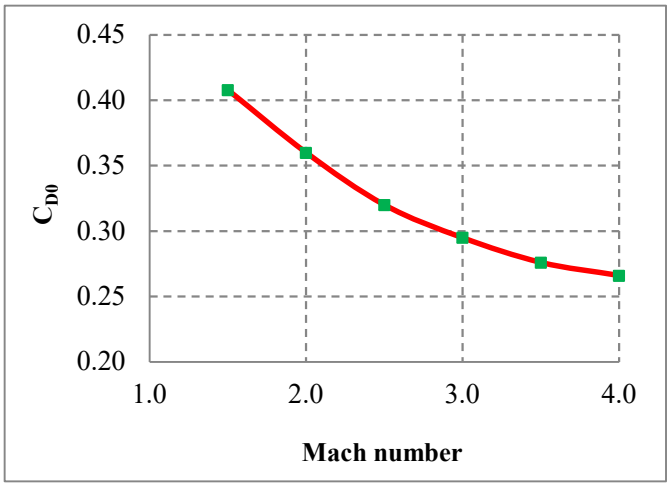

Fig. 5. Zero-yaw drag coefficient versus Mach number

Fig. 5 presents the zero-yaw drag coefficient of the projectile as a function of Mach number. An obvious trend can be seen is that C_{D0} monotonously decreases when Mach number increases. While Mach number increases from 1.5 to 4.0, the zero-yaw drag coefficient changes downwardly from 0.408 to 0.266. The total drag coefficient C_D as a function of Mach number is shown in Fig. 6 for AoA of 2^0, 4^0 and 6^0. Clearly, for any certain value of AoA, the total drag coefficient gradually decreases with the increase in Mach number. Specifically, at Mach ranging from 1.5 to 4, the total drag coefficient C_D drops from 0.436 to 0.276 for AoA of 2^0, from 0.471 to 0.291 for AoA of 4^0 and from 0.502 to 0.305 for AoA of 6^0. Conversely, it is evident that at a certain Mach number, the total drag coefficient C_D rapidly increases with the increase in AoA, for instance, at Mach number of 3.0 the coefficient C_D increases from 0.314 to 0.354 when AoA increases from 2^0 to 6^0.

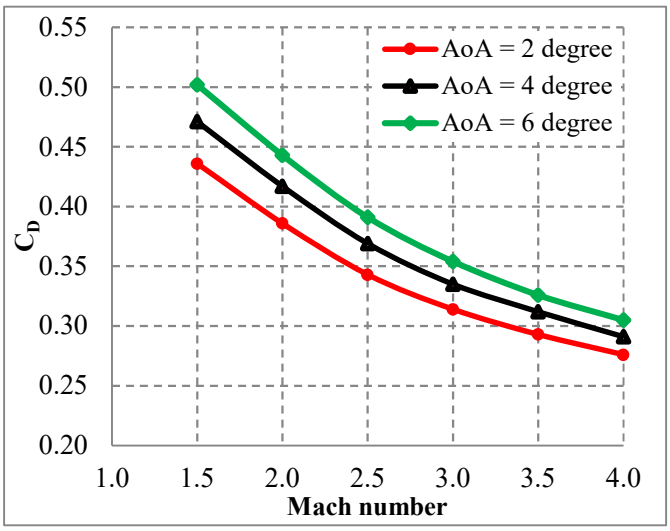

Fig. 6. Total drag coefficient versus Mach number at different AoA

The normal force coefficient $C_{N\alpha}$ and overturning moment coefficient $C_{M\alpha}$ as functions of Mach number are depicted in Fig. 7 and Fig. 8 respectively. Interestingly, the normal force coefficient behaves differently from the drag coefficients. It does not monotonously change as the later. Instead, $C_{N\alpha}$ slightly increases at first when Mach number increases to about 2.0, then decreases when Mach number continues to increase. The normal force coefficient behaves this way for all AoA investigated.

On the contrary, the overturning moment coefficient decreases monotonously with the increase in Mach number. Moreover, it is clearly shown in Fig. 8 that the overturning moment coefficient varies insignificantly with the change of AoA. Quantitatively, when Mach number increases from 1.5 to 4.0, $C_{M\alpha}$ drops from 2.450 to 1.862.

Fig. 9 and Fig.10 present the center of pressure location as functions of Mach number and AoA respectively. It can be clearly seen that for all angles of attack, the center of pressure location X_{cp} decreases with increasing in Mach number. However, the variation interval is quite narrow ranging from 1.31 to 1.41. That means the center of pressure location gradually moves

away from the center of gravity towards the projectile nose when the Mach number increases.

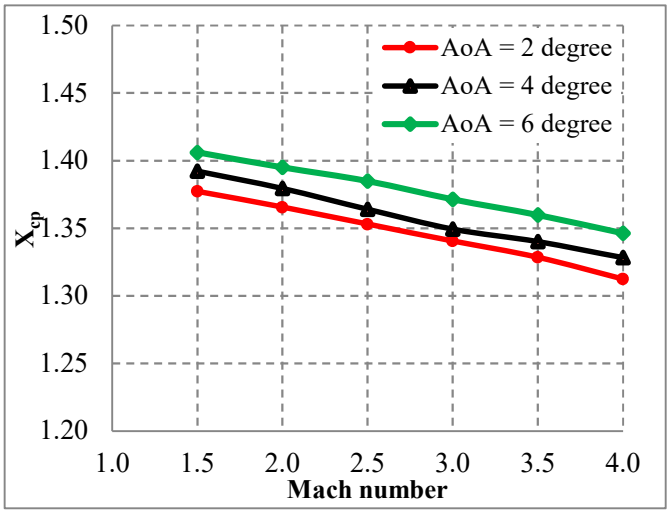

Fig. 7. Normal force coefficient versus Mach number at different AoA

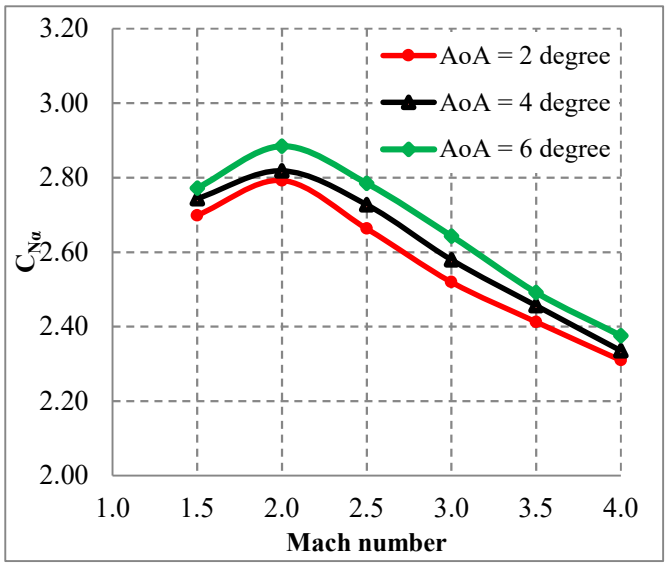

Fig. 8. Overturning moment coefficient versus Mach number at different AoA

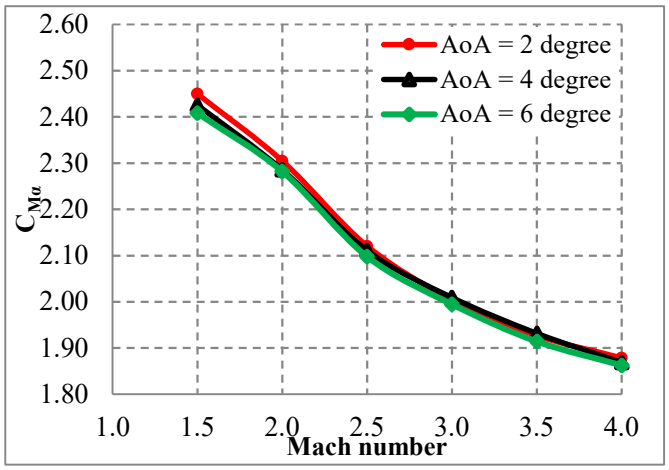

Fig. 9. Center of pressure location versus Mach number at different AoA

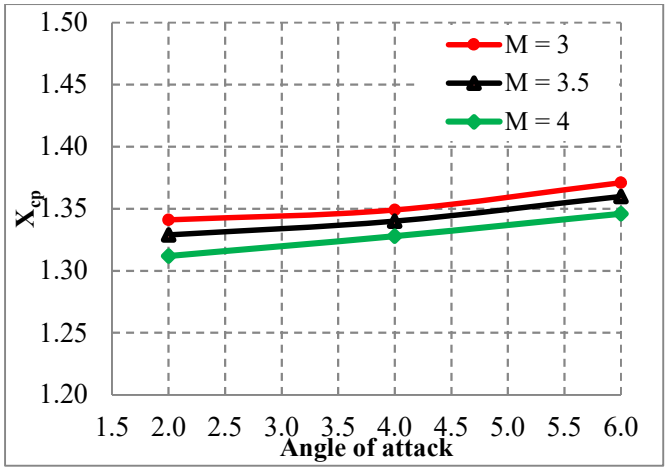

Fig. 10. Center of pressure location versus AoA at different Mach numbers

Interestingly, the opposite is observed in the Fig. 10. When the angle of attack increases, the parameter X_{cp} also increases. In other words, the center of pressure location shifts away from the projectile nose towards its center of gravity with the increase in angle of attack. These observations are consistent with that experimentally obtained by Silton and Howell for 5.56mm M855 projectile [3] as well as with results numerically obtained by Widyastuti et al. [20]. Moreover, as expected, the center of pressure is always located ahead of the center of gravity as the projectile is statically unstable.

3.2. Flow field visualization

Mach number contours of flow fields around M43 projectile at free-stream Mach number of 2.0 for different AoA are shown in Fig. 11. Obviously, the flow field at AoA of 0^0 is axisymmetric as expected. Otherwise, the flow field around the projectile exhibit asymmetry. The greater the AoA is, the more asymmetric the flow gets as seen in Fig. 11. The flow behind the projectile base is extremely complicated with reverse flow. The reverse flow gets stronger with the increase in AoA. This leads to further drop in base pressure and eventually to increasing the total drag acting on the projectile. Additionally, a strong expansion fan is formed at the boattail region where the projectile geometry undergoes an abrupt change.

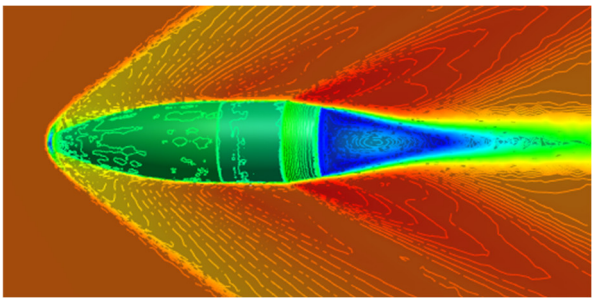

(a) AoA = 0^0

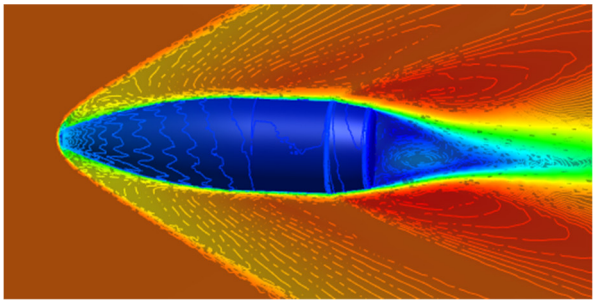

(b) AoA = 2^0

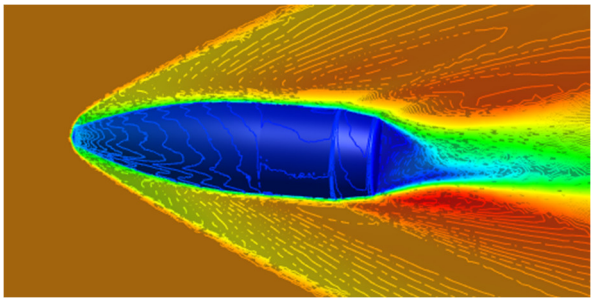

(c) AoA = 4^0

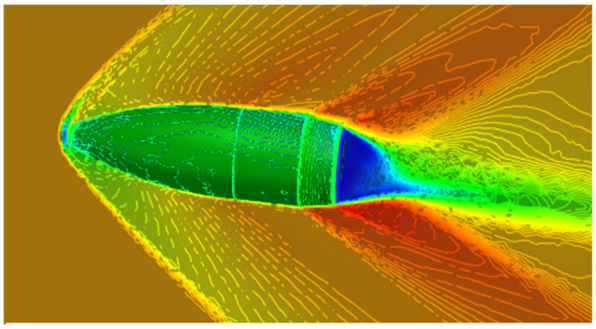

(d) AoA = 6^0

Fig. 11. Mach number contours at different AoA

4. CONCLUSION

In this study, aerodynamic characteristics of the widely used 7.62mm M43 projectile were predicted and analysed using Ansys Fluent software package with SST k-ω turbulence model. A grid independence study was carried out and the simulation results were validated against available experimental data. The computations were performed for various supersonic Mach numbers ranging from 1.5 to 4 at several small angles of attack, namely, of 0^0, 2^0, 4^0 and 6^0. The flow fields around the projectile at different AoA were also visualized and analysed. Based on the simulation results obtained in this paper, the following conclusions can be drawn:

CFD is an effective mean to study flows around a spinning projectile. The zero-yaw drag coefficient obtained using CFD method is in a very good agreement with experimental data showing the difference of only around 2.17% at Mach 2.0. Using CFD one can predict critical aerodynamic characteristics that are impossible or very difficult to obtain with experimental approach.

The zero-yaw drag coefficient and, for all angle of attack investigated, the total drag as well as overturning moment coefficients of the projectile smoothly decrease with the increasing in Mach number at supersonic flow regime. Normal force coefficient slightly increases when Mach number increases to vicinity of 2.0, then drops when Mach number continues to increase. The center of pressure location shifts in a narrow interval moving towards the projectile nose when Mach number increases and vice versa. Additionally, when the angle of attack increases, the center of pressure moves towards the projectile center of gravity and vice versa.

The findings from this research provide deeper insights into the aerodynamics of M43 projectile facilitating its application. However, for more comprehensive understanding of the aerodynamics of M43 projectile, there is a need to investigate its dynamic aerodynamic characteristics, namely, Magnus force and moment coefficients, spin damping and pitch-damping moment coefficients. That would be recommended for a continuation of this work.

REFERENCES

[1]. McCoy R., *Modern exterior ballistics: The launch and flight dynamics of symmetric projectiles*. Schiffer Military History, Pennsylvania, 2009.

[2]. McCoy R., *Aerodynamic and flight dynamic characteristics of the new family of 5.56mm NATO ammunition*. Tech. Rep. BRL-MR-3476, US Army Ballistic Research Laboratory, Aberdeen Proving Ground, 1985. Accessed: Jun. 5, 2025. [Online]. Available: https://apps.dtic.mil/sti/tr/pdf/ADA162133.pdf

[3]. Silton SI., Howell BE., *Aerodynamic and flight dynamic characteristics of 5.56-mm ammunition: M855*. Tech. Rep. ARL-TR-5182, U.S. Army Research Laboratory, Aberdeen Proving Ground, 2010. Accessed: Jun. 5, 2025 [Online]. Available: https://apps.dtic.mil/sti/tr/pdf/ADA530895.pdf

[4]. McCoy R., *The aerodynamic characteristics of 7.62mm match bullets*. Tech. Rep. BRL-MR-3733, US Army Ballistic Research Laboratory, Aberdeen Proving Ground, 1988. Accessed: Jun. 5, 2025. [Online]. Available: https://apps.dtic.mil/sti/tr/pdf/ADA205633.pdf

[5]. Maynard JP., *Aerodynamic characteristics of the 7.62mm NATO ammunition M-59, M-80, M-61, M-62*. Tech. Rep. No. 1833, US Army Ballistic Research Laboratory, Aberdeen Proving Ground, 2010. Accessed: Jun. 5, 2025. [Online]. Available: https://apps.dtic.mil/sti/tr/pdf/AD0815788.pdf

[6]. McCoy R., *The aerodynamic characteristics of .50 ball M33, API, M8, and APIT, M20 ammunition*. Tech. Rep. BRL-MR-3810, US Army Ballistic Research

Laboratory, Aberdeen Proving Ground, 1990. Accessed: Jun. 5, 2025. [Online]. Available: https://apps.dtic.mil/sti/pdfs/ADA219106.pdf

[7]. Silton SI., *Navier-Stokes computations for a spinning projectile from subsonic to supersonic speeds*. Tech. Rep. ARL-TR-2850, U.S. Army Research Laboratory, Aberdeen Proving Ground, 2002. Accessed: Jun. 5, 2025. [Online]. Available: https://apps.dtic.mil/sti/pdfs/ADA407616.pdf

[8]. Silton SI., "Navier–Stokes computations for a spinning projectile from subsonic to supersonic speeds," *Journal of Spacecraft and Rockets*, 42/2, 223-231, 2005. https://doi.org/10.2514/1.4175

[9]. Silton SI., "Navier-Stokes predictions of aerodynamic coefficients and dynamic derivatives of a 0.50-cal projectile," in *29th AIAA Applied Aerodynamics Conference*, American Institute of Aeronautics and Astronautics, 2011. https://doi.org/10.2514/6.2011-3030

[10]. DeSpirito J., Plostins P., "CFD prediction of M910 projectile aerodynamics: Unsteady wake effect on Magnus moment," *AIAA Atmospheric Flight Mechanics Conference and Exhibit,* American Institute of Aeronautics and Astronautics, 2007. https://doi.org/10.2514/6.2007-6580

[11]. DeSpirito J., "CFD aerodynamic characterization of 155-mm projectile at high angles-of-attack," in *35th AIAA Applied Aerodynamics Conference*, American Institute of Aeronautics and Astronautics, 1-20, 2017. https://doi.org/10.2514/6.2017-3397

[12]. Ferfouri A., Allouche T., Jerkovic D., Hristov N., Vuckovic M., Benmeddah A., "Prediction of drag aerodynamic coefficient of the 155 mm projectile under axisymmetric flow using different approaches," *Journal of the Serbian Society for Computational Mechanics,* 17/2, 69-86, 2023. Available: https://doi.org/10.24874/jsscm.2023.17.02.06

[13]. Sertkaya A., Caliskan C., Neseli S., "Comparison of real and simulation aerodynamic coefficients for 155mm ammunition using open-source code SU2 software," *Journal of Polytechnic,* 25/ 4, 1835-1845, 2022. https://doi.org/10.2339/politeknik.1133519

[14]. Albisser M., *Identification of aerodynamic coefficients from free flight data*. PhD Thesis, University of Lorraine, Nancy, France, 2015.

[15]. Suliman MM., *Computational investigation of missile aerodynamic characteristics*. PhD Thesis, Military Technical College, Cairo, Egypt, 2010.

[16]. Braun WF., *Aerodynamic data for small arms projectiles*. Tech. Rep. BRL R 1630, US Army Ballistic Research Laboratory, Aberdeen Proving Ground, 1973. Accessed: Jun. 5, 2025. [Online]. Available: https://babel.hathitrust.org/cgi/pt?id=mdp.39015095102698&seq=55

[17]. Menter FR., "Two-equation eddy-viscosity turbulence models for engineering applications," *AIAA Journal,* 32/ 8, 1598-1605, 1994. https://doi.org/10.2514/3.12149

[18]. Matsson JE., *An introduction to Ansys Fluent 2023*. SDC Publications, Kansas, 2023.

[19]. Salunke S., Shinde S., Gholap T., Sahoo D., "Comparative computational analysis of NATO 5.56mm, APM2 7.62mm and AK-47 7.82mm bullet moving at Mach 2.0 in close vicinity to the wall," *FME Transactions*, 51/1, 81-89, 2023. http://doi.org/10.5937/fme2301081

[20]. Widyastuti R., Kusuma R., Rochiem R., Pramujati B., "Center of pressure analysis for bullet angle of attack using computational fluid dynamic," in *AIP Conference Proceedings*, 2384/1, 2021. https://doi.org/10.1063/5.0071491